Meeting overlay requirements for future technology nodes with in-die overlay metrology

Bernd Schulz*[a], Rolf Seltmann[b], Jens Busch[a], Fritjof Hempel[b], Eric Cotte[c], Benjamin Alles[d]
[a]AMD Saxony LLC & Co. KG, Wilschdorfer Landstrasse 101, D 01109 Dresden;
[b]AMD Fab36 LLC & Co. KG, Wilschdorfer Landstrasse 101, D 01109 Dresden;
[c]AMTC GmbH & Co. KG, Rähnitzer Allee 9, D 01109 Dresden;
[d]University of Technology Munich, Boltzmannstr. 3, D 85748 Garching

ABSTRACT

As a consequence of the shrinking sizes of the integrated circuit structures, the overlay budget shrinks as well. Overlay is traditionally measured with relatively large test structures which are located in the scribe line of the exposure field, in the four corners. Although the performance of the overlay metrology tools has improved significantly over time it is questionable if this traditional method of overlay control will be sufficient for future technology nodes. For advanced lithography techniques like double exposure or double patterning, in-die overlay is critical and it is important to know how much of the total overlay budget is consumed by in-die components.

We reported earlier that small overlay targets were included directly inside die areas and good performance was achieved[1]. This new methodology enables a wide range of investigations. This provides insight into processes which were less important in the past or not accessible for metrology. The present work provides actual data from productive designs, instead of estimates, illustrating the differences between the scribe line and in-die registration and overlay.
The influence of the pellicle on mask and wafer overlay is studied. Furthermore the registration overlay error of the reticles is correlated to wafer overlay residuals.
The influence of scanner-induced distortions (tool to tool differences) on in-die overlay is shown.
Finally, the individual contributors to in-die-overlay are discussed in the context of other overlay contributors and are compared with the available overlay budget. It will be shown that new overlay correction schemes which take advantage of the additional in-die overlay information need to be considered for production.

Keywords: in-die overlay, metrology, residuals, process control.

1. INTRODUCTION

Historically, DRAM and more recently Flash memory devices have been the drivers of semiconductor technology. In particular, overlay accuracy has always been at the edge for DRAM manufacturing. With the advent of double patterning scenarios, the concerns with respect to the control of overlay grow dramatically.
In contrast to DRAM production, overlay has not been a major area of concern for production of logic devices thus far. With the steep increase of on-chip cache memory in state of the art microprocessor designs and the resulting need of minimization of the individual SRAM-cells, the overlay-requirements are suddenly similar to those of DRAMs and are thus becoming a completely new challenge for engineers in microprocessor manufacturing.
It is well known that the very tight overlay specifications for 45nm and 32nm technology nodes are extremely challenging[2]. Sources of overlay error which were tolerable until now might become critical and therefore need special attention. The individual contributors to the total overlay error budget have been classified and measured or estimated in the past in various studies[3, 4].
Besides scanner lenses, stages and alignment mark quality, the impact of reticle registration on the overall overlay budget comes more and more into the focus of the work[5, 6]. As Lee et al. and Doh et al. concluded, reticle-to-reticle overlay is responsible for about 25% of the wafer overlay error[6, 7]. However, this number depends heavily on the degree of process control of both the reticle and wafer manufacturing. State of the art mask shops are fully aware about that challenge and work hard to decrease the registration of the reticle. However, the transfer of the reticle registration onto the wafer has not yet been fully explored on production reticles[7]. This situation is mainly a result of the fact that currently mask registration and wafer overlay are measured on different structures and in different locations. It must be checked if this

*bernd.schulz@amd.com; phone: 49 351 277-2544; fax: 49 351 277-92544

induces additional errors. In our study, we attempted to explore the transfer of the reticle registration onto the wafer and its context to other sources of intra-field overlay. Furthermore, we compared reticle-to-reticle overlay and wafer overlay for a group of reticles from different mask shops, thus generating data for an overlay error budget.

2. METHODOLOGY

2.1 Wafer preparation and metrology

For the measurement of in-die overlay directly on product wafers, micro AIM (advanced imaging metrology) overlay targets with a 1X size of 13x13 µm² were inserted in the layout of successive lithography layers within the actual die, in multiple locations across the reticle field[1]. Insertion locations were selected in areas of the device without electrical functionality. These areas are typically filled with dummy tiles, and some of the dummy tiles are removed to place the overlay marks. Beside the in-die micro AIM targets, all reticles contained the normal box-in-box, standard size AIM as well as micro AIM overlay targets in the four corners of the scribe line. Fig. 1 shows the optical image of a normal size AIM target compared to a micro target at poly gate, at the same magnification.

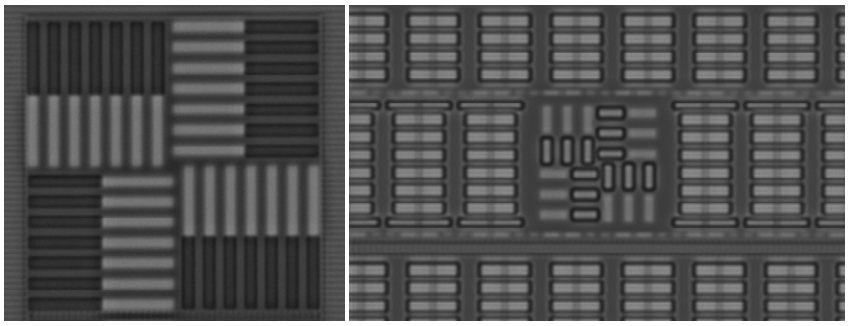

(a) (b)

Fig. 1: Optical image of (a) a standard AIM, and (b) 3-bar micro AIM overlay target (FOV 50µm).

The design of the 3-bar micro AIM target is shown in Fig. 2. In the reference layer the target was built as a so called simultaneous target with a segmented inner part and a non-segmented outer part. This special layout was chosen for the combination of the shallow trench isolation (STI) layer and the poly gate layer. With this design, the target can be used for pattern placement measurements at the reference layer. After completion of the wafer processing up to the poly gate layer masking step, it can be used as a normal non-segmented micro AIM target. The segmentation of the inner part does not negatively influence the optical image at the poly gate resist mask as long as the segmented inner part is fully covered by poly silicon and resist. This fact is limiting the dynamic range of the special micro overlay target to a certain degree compared to the standard design targets. The in-die overlay experiments were conducted on production and short-loop wafers. The overlay of the production wafers was controlled by a closed-loop APC controller and was small enough to fall into the reduced dynamic range of the target. In the case of short-loop wafers with manual overlay correction, special care was taken to avoid too large overlay errors.

For the comparison of scribe line to in-die overlay, short-loop and production wafers were exposed on a single exposure tool (ASML TwinScan XT1250). Due to the layout of the overlay targets, a resist-in-resist process could not be used for the short-loop wafers. Therefore the reference layer in the short-loop wafer process was etched as an approximately 120nm deep trench into bulk silicon. The second layer was exposed on top of this structure using a BARC coating underneath the ArF resist layer. The production wafers were processed according to the normal process flow, but the two layers of interest were exposed on a single exposure tool.
All overlay measurements were performed on a single KLA-Tencor Archer AIM+ tool in order to avoid additional measurement errors due to tool-to-tool matching. Special recipes were created using the ARC (automatic recipe creation) function, which include the scribe line standard AIM targets, the scribe line micro AIM targets and all in-die micro targets.

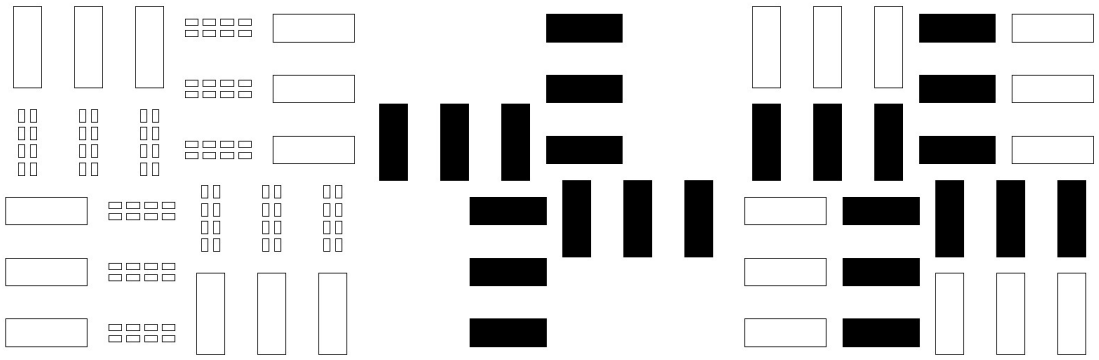

(a) (b) (c)

Fig. 2: Layout of micro AIM target: (a) simultaneous target layout for STI, (b) layout for poly gate, and (c) resulting micro AIM overlay target at poly gate. In black are the structures from poly gate, and in white are the structures from the STI layer.

During a first run, the recipes went through the automatic optimization process with OMC function (optimal measurement condition) enabled. Individual TIS correction was done for all target locations in the recipe. It should be mentioned here that the required overlay tool recipe quality was achieved only when all three software features (ARC, OMC, TIS on array) were used together. The correlation values between reticle and wafer overlay increased significantly when OMC was activated for recipe optimization. For simpler comparison to production sampling plans, the same fields (9 per wafer) were selected as sampling plan in all experiments.

2.2 Reticle registration measurements

In this investigation, only sets of reticles previously or currently used for production of different 90nm design rule logic devices were included. A Vistec IPRO 3 was employed to obtain registration data on both reticles of each set. The reticle registration measurement was performed in a way that mimics the wafer overlay measurements, by measuring on the reticles the exact same features that are used by the KLA-Tencor wafer overlay metrology tool. Thus, instead of basing reticle registration on IPRO crosses, as it is done on most products, the placement of the in-die micro AIM targets was studied, as well as scribe line micro AIM and standard AIM targets. Fig. 3 (a) is one example distribution of the measurement locations (white crosses) throughout the reticle. The two arrows (left and right) in each of the four corners point to the locations of the standard size and micro AIM targets in the scribe line, respectively. The total number of measurement points per reticle set was between 52 and 86, depending on the reticle set. The registration measurement on the micro AIM structures is schematically shown in Fig. 3 (b) and (c): for the measurements on the reference layer reticle the outer features (b) and for the measurements on the current layer reticle the inner features (c) were used.

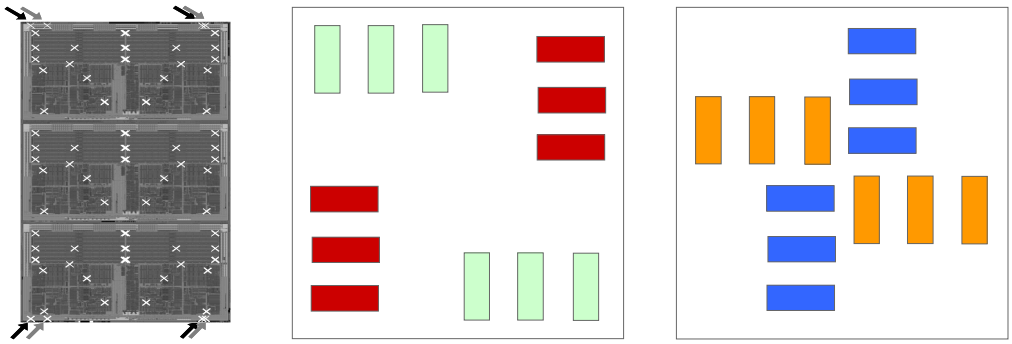

(a) (b) (c)

Fig. 3: (a) reticle registration measurement locations and schematic of micro AIM targets (b) outer and (c) inner features.

The X-position of the micro AIM marks was obtained by averaging the placement of the 6 vertical lines, and the Y-position via the 6 horizontal lines, in an effort to calculate reticle-to-reticle overlay in a manner similar to the wafer overlay measurement. A similar approach was used for standard AIM targets. The IPRO recipes had to be created manually due to the non-standard character of all the structures.

The following nomenclature for the reticle names will be used throughout this article: each reticle name is comprised by product (1,2,3), layer (L1-L4) and reticle revision (A1-C1). The names of the reticle pairs are given by product, layer and reticle revision of the reference layer followed by layer and reticle revision of the actual layer. Most of the work focuses on layer L1 and L2, which represent the reticles for shallow trench isolation (STI) and poly gate, respectively. Layer L3 and L4 represent a metal and a via layer.

3. RESULTS

3.1 Registration error and reticle-to-reticle overlay

The result of the standard registration measurements in the scribe lines (3s, spec), which is an important quality parameter of a reticle as it is used to verify that it meets its specifications for 3-sigma registration, is compared in Fig. 4 to the result of the special reticle registration measurements on in-die overlay structures (3s, in-die). All registration measurements are corrected for magnification and non-orthogonality. The standard registration measurement results of all reticles vary in a range from 8 to 17nm in the scribe line. The first two reticles highlighted with the box were manufactured with an older generation mask write tool, which explains the relative high 3-sigma in-die registration error.

In contrast to the standard registration measurement the in-die registration of all other reticles is smaller and less than 8nm. This is mainly caused by the order in which the different parts of the reticle are written: the die or dies get written first, followed by the surroundings, such as the outer scribe lines. If the scribe line structures were written in the same run as the chip, this would improve their placement, and the scribe line registration would be more meaningful. The difference in pattern density in the scribe line compared to the die should also be noted[6]. In other words, judging the quality of a reticle by the standard registration measurements in the scribe line is not representative at all of the placement of the structures in the die. This situation can only be improved when the specification of reticle registration error is based on a higher sampling plan including representative structures and especially locations within the die.

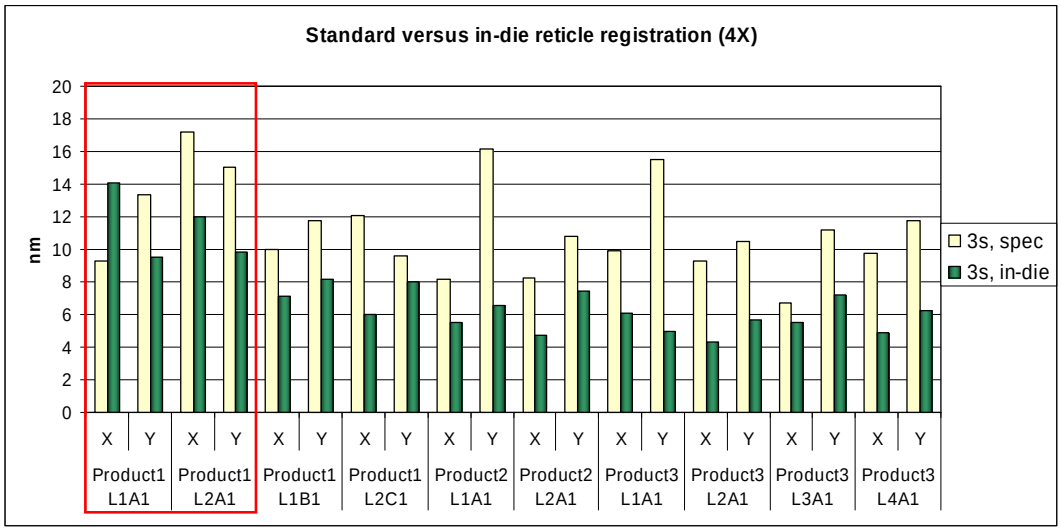

Fig. 4: Reticle registration results (4X) from different reticles measured on standard IPRO crosses and on in-die micro AIM targets as described.

Fig. 5 shows the corresponding reticle-to-reticle overlay error for the standard registration measurement (3s, spec), the registration of all available overlay structures (3s, all) and the registration of the in-die overlay structures only (3s, in-die), calculated as the difference between the registration errors of the two reticles in the set. The reticle pairs, which include at least one reticle from an older write tool (highlighted with box and doted box), show also a higher mask-to-mask overlay error. In contrast to the registration values, the differences between standard and in-die reticle-to-reticle overlay vary significantly from reticle set to reticle set.

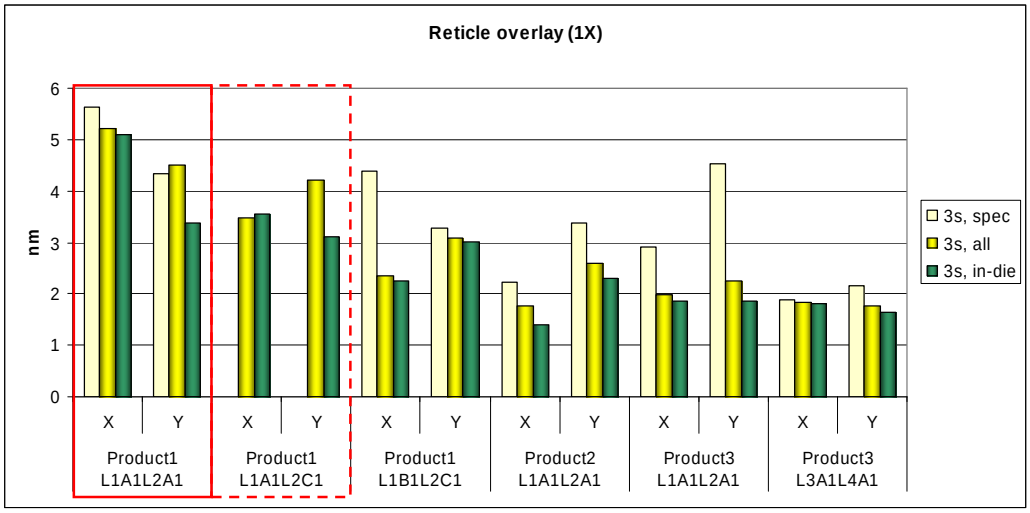

Fig. 5: Reticle-to-reticle overlay (1X) results from different reticle pairs measured as specified (spec), on all standard and micro AIM targets (all), and micro targets in-die only (in-die).

The reticle-to-reticle overlay error depends on the correlation between the registration errors of two reticles[7]. When the registration errors are fully correlated (correlation coefficient r = 1), the mask-to-mask overlay is perfect. The reticle-to-reticle overlay is worst in the anti-correlated case (r = -1, illustrated in Fig. 6), and randomly distributed in the non-correlated case (r = 0). Lee et al. therefore proposed to take the mask-to-mask overlay error (or the level of correlation between registration errors) into account for the quality assessment of reticle sets for critical layer combinations (for double exposure technique – DET, or double patterning technique - DPT), which could relax the registration requirements, especially in the case of positive correlation. It is obvious from Fig. 5 that the sampling size and the locations of the standard registration measurement in the scribe lines are also not representative enough to be used for an estimate of the correlation level between the reticles, pointing again to the need for in-die measurements.

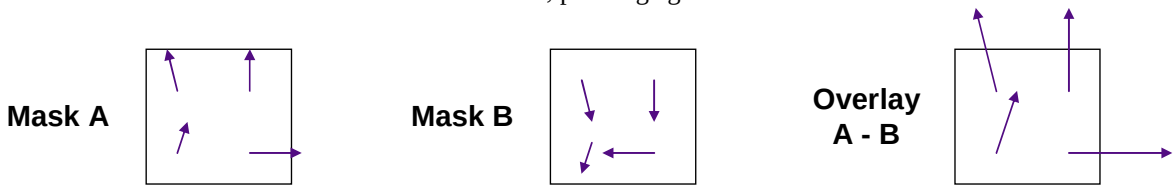

Fig. 6: Anti-correlated registration errors on mask A and B leading to the worst case of mask-to-mask overlay error.

3.2 Pellicle influence on reticle-to-reticle overlay

Reticles L1A1 and L2A1 from the Product3 set were used to study the effect of different pellicles on the reticle-to-reticle overlay error. The first registration measurement on in-die overlay structures was performed with the existing pellicles. Then these pellicles were removed and a second registration measurement was done without pellicle. In a next step new pellicles were mounted and a third registration measurement took place. The effect of the pellicles was calculated as the difference between the measurements with and without pellicle respectively. The vector maps of the differences in mask-to-mask overlay are shown in Fig. 7 (4X). No systematic pattern can be seen, which might be related to relative sparse sampling across the reticle field. At wafer level the contribution of the pellicle, expected to be approximately 1nm 3sigma, was too small to be detected with the given methodology and precision levels of the overlay metrology.

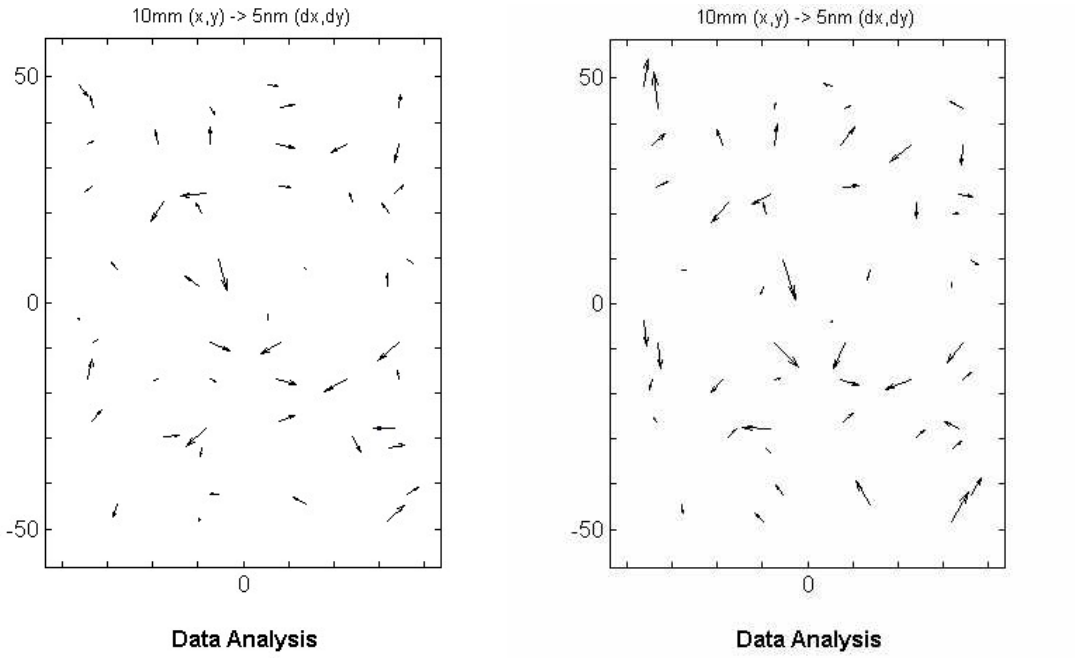

Fig. 7: Mask-to-mask overlay error introduced by different pellicles: (a) old pellicle set, (b) new pellicle set (4X).

3.3 Scribe line versus in-die wafer overlay

Overlay errors can be decomposed by modeling into different terms. The systematic terms can be used to correct (reduce) the overlay error on the wafer. The residual from the model is the non-correctable part of the overlay error. Residuals should be ideally close to zero and randomly distributed. When overlay is measured in many locations per field, the residual distribution across wafer and fields actually exhibits a large systematical portion.

In order to compare the quality of different overlay correction scenarios (standard: scribe line 4 corner measurements vs. a combination of scribe line and in-die overlay, or exclusively in-die overlay measurements) the overlay results were analyzed with a standard 10-parameter ASML scanner model[8]. The data was processed with KT Analyzer in three different analysis sets: the first set included only the standard size scribe line AIM targets (representing the normal production use case), the second set included all available targets and the third set included only the in-die micro targets. The comparison of the 3 sigma residuals of the three analysis sets is shown in Fig. 8 for normal production lots with different product layouts. Layers L1 and L2 were always exposed with the same reticle pair for each product on the same single exposure tool (indicated in the chart). Short-loop wafers were used for the reticle set from product 3. It can be seen that the residuals from all analysis sets are in the range from 3nm to 7nm.

The absolute difference of the residuals, noted as abs(Res 3s delta), and the maximum predicted overlay error between analysis sets 1 and 2, noted as abs(MPError delta), are shown in Fig. 9. Although the differences in residuals of the three products are below 1nm the differences of the maximum predicted overlay error are not small enough to be ignored in future technology nodes. This indicates that the result of the modeling depends on the number and the spatial distribution of measurement points in the sampling set. It also shows that, as in the case of the scribe line registration measurements, the overlay measurement in the scribe line is not representative enough of the whole die area and can introduce significant overlay errors when only this data is used for overlay correction.

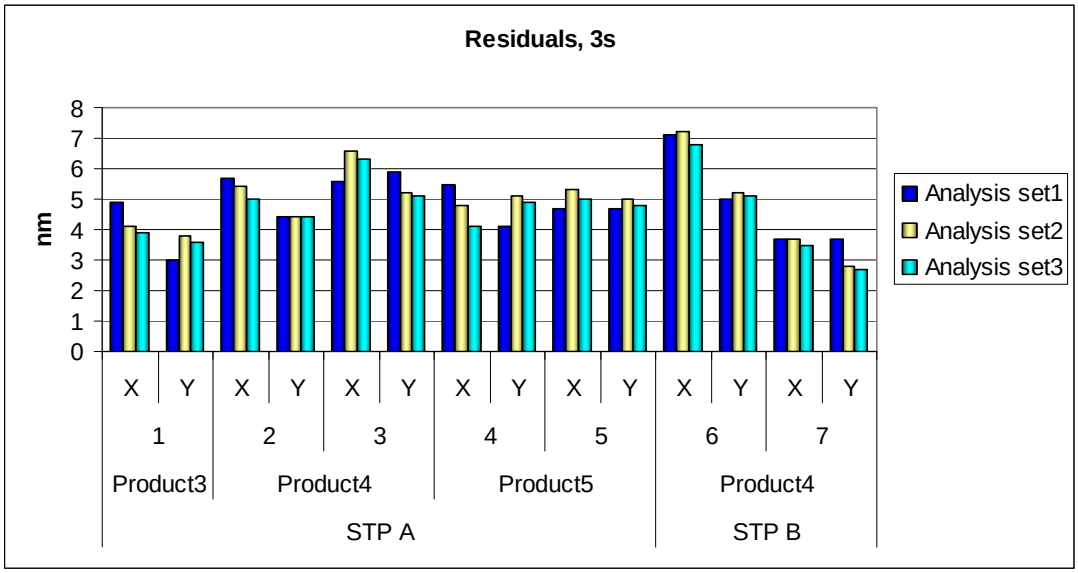

Fig. 8: Comparison of residuals (1X) for three different analysis sets (set1- standard AIM targets in 4 corners, set2- all targets, set3- only in-die targets) for different products and wafer lots.

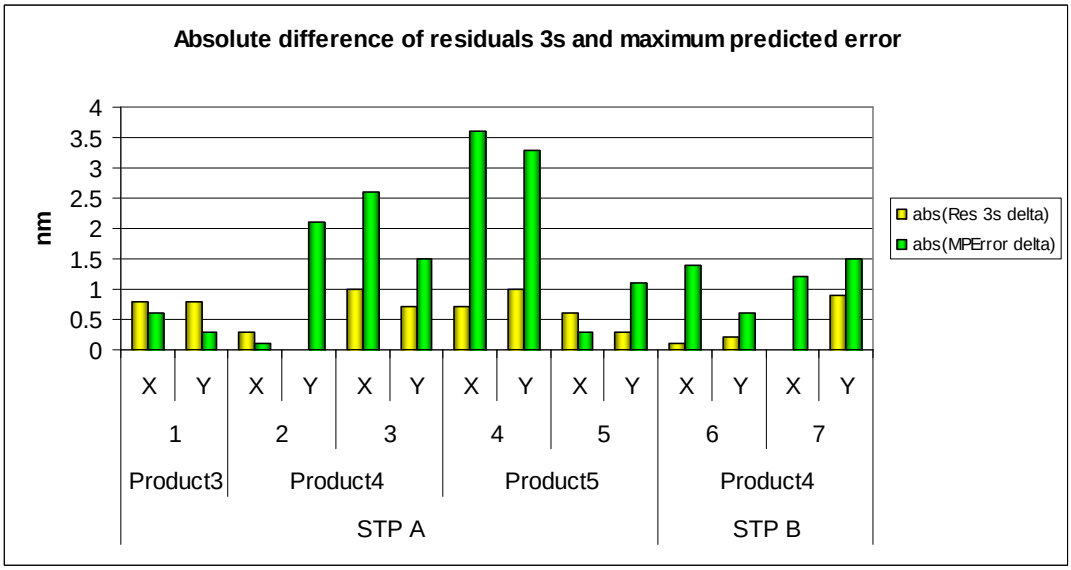

Fig. 9: Absolute differences of residuals and the maximum predicted OVL error between analysis set 1 (4 corners) and 2 (all targets) for different products and wafer lots (1X).

3.4 Correlation of wafer overlay residuals to reticle-to-reticle overlay

Although the statistical concept of overlay mark fidelity was developed for overlay marks printed in close proximity, some of the ideas are useful when the correlation of wafer overlay to reticle-to-reticle overlay is studied[9]. If the targets are not in close proximity but distributed across the reticle field, the assumption that all targets produce the same overlay results is no longer valid. Therefore one has to apply a linear (inter- and intrafield) overlay model to the overlay values and should replace the overlay values in the calculation with the respective residual values for each target.
The contribution of the reticle should be present in every field on the wafer. The best way to extract this information, which is constant for all fields, is to calculate the average of all *X* (respectively *Y*) overlay residual values in each

location *i* across all fields *j*, where *i* is the index of the overlay target out of *N* overlay targets in the field and *j* is the index of the field number out of *F* fields:

$$\overline{res_i} = \frac{\sum_{j=1}^{F} res\_X_{ij}}{F} \quad (1)$$

The attempt to correlate wafer overlay to mask-to-mask overlay clearly reveals the current limitations of the methodology and the available metrology in respect to precision and signal to noise ratio. The main disadvantage of using average field residuals as defined in equation 1 is that any process-related non-linear across-wafer effect influences the average field residual. Therefore one cannot expect a 1:1 transfer of reticle error to the wafer in this case. A good way to check for such process effects is for example to plot the residuals versus the wafer radius. Only if the residuals change very little along the radius can the slope of the correlation be expected to be close to one. Another reason for imperfect correlation is the presence of aberation-related pattern placement error (PPE). Since the micro AIM target was designed with device-like structure size, it is sensitive to PPE and the measured overlay is the sum of the overlay and the PPE. This needs to be taken into account when the correlation of reticle and wafer overlay is studied.

Commercially available overlay analysis software packages currently do not have the capability to deal with reticle registration or reticle-to-reticle overlay data. Therefore a data-handling software and a mathematical concept of an empirical model of mask placement error transfer during exposure was developed by one of the co-authors[10]. The result of the model is shown in Fig. 10, where DX-DX pertains to the correlation of the overlay error in the X direction on mask (x-axis) and wafer (y-axis) in nm at mask level, DY-DY to data in the Y direction, and DX-DY and DX-DY represent the cross-terms. Of particular interest are the shared variance values (R^2), which are representative of the correlation between the mask and wafer data set: $R^2 = 0$ for uncorrelated sets, and $R^2 = 1$ for fully correlated or anti-correlated sets. The sign of the correlation coefficient R indicates that the data is positively correlated, and the R^2 values indicate that the correlation between mask and wafer overlay error is very good.

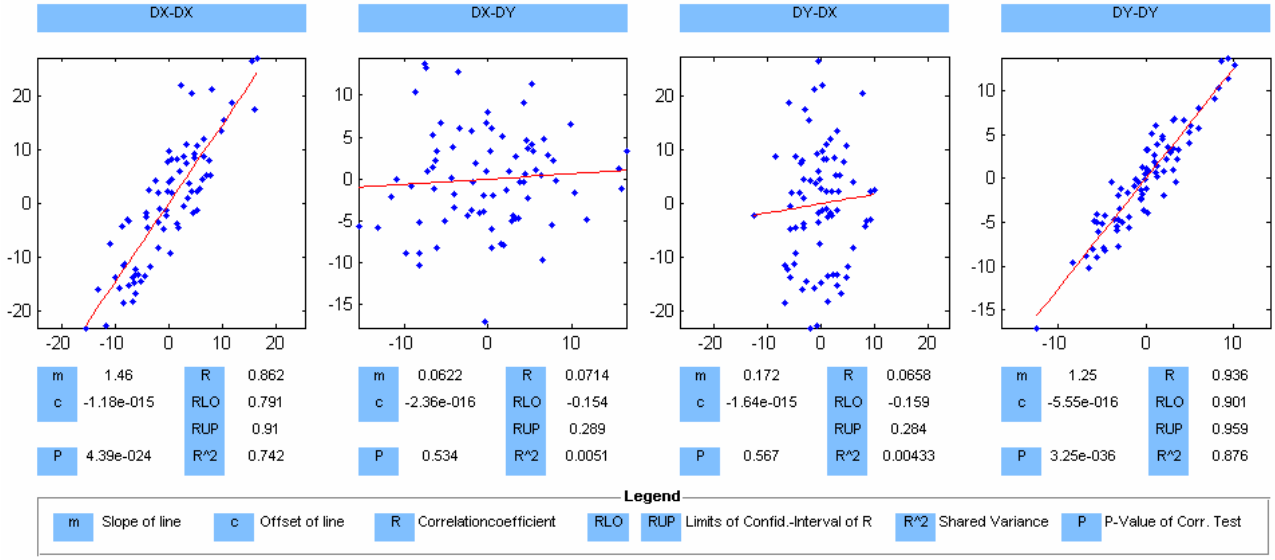

Fig. 10: Correlation of reticle registration overlay to wafer overlay (4X) for product 1 reticle set L1A1-L2A1.

Besides the correlation coefficients, the values of the slopes are indicative of the correlation or lack thereof: the slopes are close to 0 for the cross-terms, as can be expected. The slopes are greater than one for the placement error transfer in both X and Y directions, which can be explained when the reticle-to-reticle overlay, shown in Fig. 11(a), is subtracted from the wafer overlay, plotted in Fig. 11(b). The vector map resulting from the subtraction of mask-to-mask overlay from wafer overlay, in Fig. 11(c), shows the combination of exposure tool contribution and measurement tool noises. Further work is needed to study the factors that influence the remaining difference between average residual error and mask-to-mask overlay.

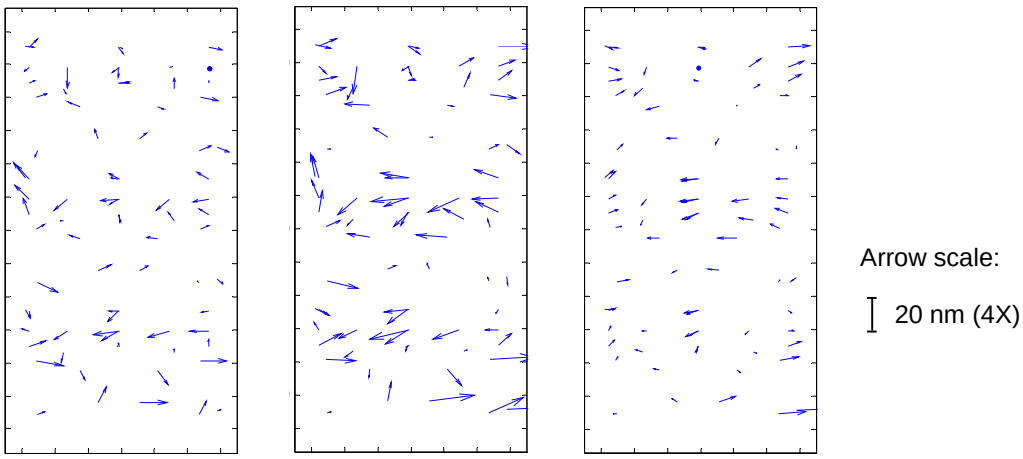

Fig. 11: Vector map of (a) reticle-to-reticle overlay, (b) wafer overlay, and (c) tool-induced distortions (same scale for all plots, 4X).

3.5 Scanner matching influence

For the study of scanner matching, production lots from Product4 and Product5 were used. Reference overlay data was generated by exposing both layers of Product5 on a single exposure tool, STP A, and both layers of Product4 on STP B. These results were compared to lots for which layer L1 was printed on the reference scanner while layer L2 was printed on scanner STP C. In order to quantify the systematic contributors to the total residual error, the overlay was measured on all available scribe line and in-die overlay targets, as described in section 2.1 and modeled in two different ways: in one model (composite field), the intra-field model is determined using the intra-field data averaged over all measured fields, and in the second model (field-by-field), the intra-field model is allowed to vary by field. The difference in the residuals between the two models is an estimator of the unmodeled systematic field-to-field bias[4]. A further breakdown of this bias into a process- and scanner-induced part is not directly possible with the data set used, but it can be assumed that the process-induced systematic residual component is the same for all lots in the experiment since they were manufactured with an identical process flow. Finally, the average field residuals (which are identical for both modeling methods) were calculated as an estimator of the residual component, which is constant for all fields. The results are shown in Fig. 12. In the case of single machine overlay, the wafer residuals are small, as expected. The difference between the composite and the field-by-field model is also small, but a difference between STP A and STP B can be noted. The average field residuals (sum of reticle-to-reticle overlay and PPE) contribute between 50% and 70% to the total residual error. One can assume that for DET or DPT processes with tighter overlay and CD uniformity specifications a single machine exposure scenario will be the best solution. In this case, the overlay contribution of the reticle is the dominating component. This emphasizes the necessity of better sampling for registration and overlay metrology, as mentioned in Sections 3.1 and 3.3, and the need to manufacture positively-correlated reticle sets for the overlay-critical layers. For the case of mixed-machine overlay, the wafer residuals of the composite field model are significantly higher compared to the field-by-field model and the average field residuals stay almost the same. The contribution of the average field (reticle-to-reticle overlay plus difference in lens distortions) is reduced to between 35% and 55%. The majority of the total residual must be related to the imperfect matching of the stage grids. Different scanner vendors are aware of this source of overlay error and are working on solutions to improve this situation[11]. This example shows that with a relatively small data set obtained from in-die overlay measurements it is possible with the proposed methodology to get quantitative measures of stage grid error (difference between the two modeling methods) and lens distortion differences (differences in average field residuals). From Fig. 12, it can be concluded that the stage grid matching of STP A and STP C is not perfect, whereas the lens distortion differences are slightly higher for the combination STP B to STP C.

Guidelines for future overlay and registration specifications can be derived more easily when in-die overlay results are analyzed in the proposed way and compared to reticle registration and reticle-to reticle overlay[10].

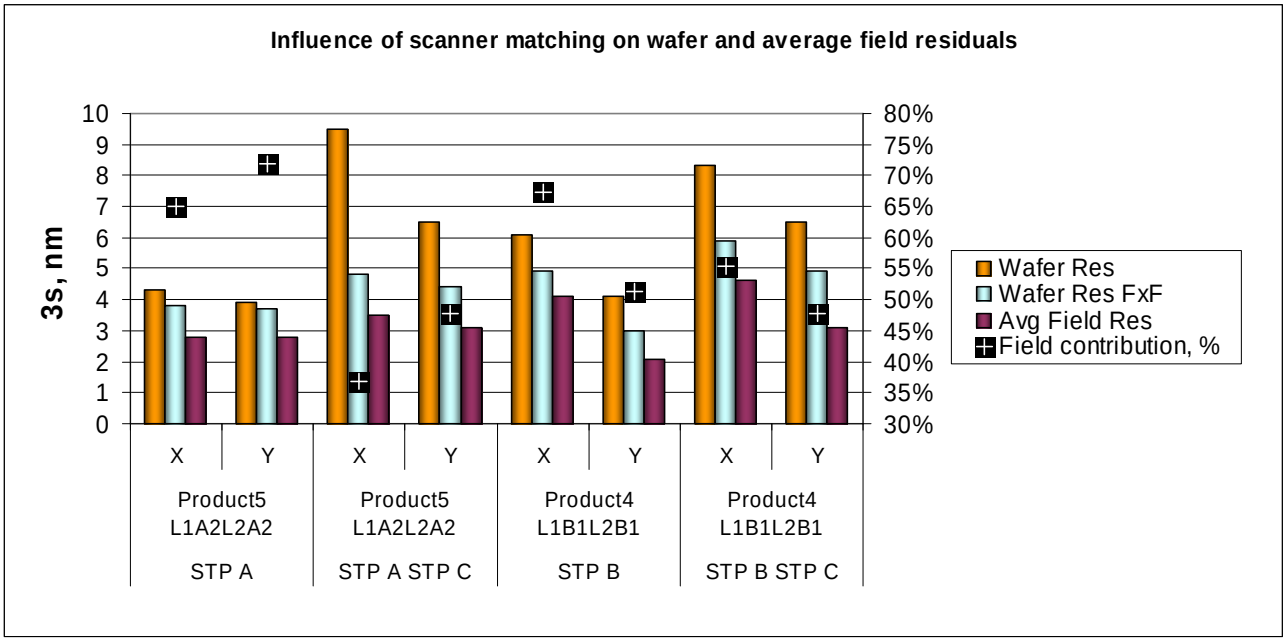

Fig. 12: Influence of scanner matching on wafer residuals for a composite field model (Wafer Res), a field-by-field model (Wafer Res FxF) and average field residuals (Avg Field Res).

4. CONCLUSIONS

It was shown that the current way to measure and specify reticle registration and wafer overlay does not correspond well with the requirement to be representative of the whole reticle area. Therefore, in-die test structures suitable for registration and overlay measurement need to be included in future product layouts. The quality assessment of reticles should be based on a higher sampling rate for registration measurements including die-area targets. It was shown that in-die overlay measurements provide a better modeling for scanner corrections than scribe-line targets.

The correlation between reticles should be taken into account for overlay-critical layer combinations, especially since the reticle contribution dominates when single machine exposure scenarios are used for production. Optimal overlay sampling plans need to be developed, which take into account the individual fingerprints of reticle pairs used for the exposure. The transfer of reticle registration errors to the wafer was studied on production plates, and a very good correlation was found, pointing to the importance of reticle registration in the overall wafer overlay budget. However, the limited amount of data collected did not make it possible to derive a complete and statistically sound error budget.

Since the AIM and micro AIM targets were non-standard for registration, recipes had to be created by hand, which should be avoided in the future, as automatic recipe creation and optimization helps to avoid human errors when recipes with many sites need to be set up. For the required levels of overlay control, sub-nanometer precision for overlay and registration metrology on small in-die test structures will be necessary for future lithography nodes. Metrology tools with higher intrinsic resolution (CDSEM) or precision (scatterometry-based overlay) could be used in addition or as alternative to image-based overlay metrology to better characterize the influence on overlay of reticles, scanner lenses, and process steps. The capabilities of current overlay analysis software packages should be improved significantly, including easy-to-use import and export functions for non-standard overlay data sources (CDSEM) and registration data.

Although data handling was made in a semi-manual fashion and metrology tools showed their limitations, it was possible to reach conclusions on the better suitability of in-die overlay measurements for reticle assessment and scanner correction modeling. More work is needed to better understand how the registration of reticles can be improved and what contributes to the remaining differences between average field residuals and reticle-to-reticle overlay, and therefore to the overall wafer overlay error budget.

ACKNOWLEDGEMENTS

The authors would like to thank Christian Sparka from KLA-Tencor for providing valuable input on overlay measurement improvement as well as Jens Rudolf and Gunther Antesberger of AMTC for some help in setting up reticle registration recipes. AMTC is a joint venture of Infineon, AMD and Toppan Photomasks.
AMD and AMTC gratefully acknowledge the financial support of the Federal German Ministry of education and Research (BMBF) under Contract No. 01M3154A ("Abbildungsmethoden fuer nanoelektronische Bauelemente").

REFERENCES:

1. B. Schulz, R. Seltmann, J. Paufler, P. Leray, A. Frommer, P. Izikson, E. Kassel, M. Adel, "In-chip overlay metrology in 90nm production", ISSM2005 Conference Proceedings, 390-393 (2005)
2. ITRS-Roadmap, 2005 edition, http://www.itrs.net/
3. M. Adel, A. Frommer, E. Kassel, P. Izikson, P. Leray, B. Schulz, "In field overlay uncertainty contributors – a backend study", Proc. SPIE 6152, 615213 (2006)
4. A. Frommer, E. Kassel, P. Izikson, M. Adel, P. Leray, and B. Schulz, "In field overlay uncertainty contributors", Proc. SPIE 5752, 51 (2005)
5. E. Cotte, B. Alles, T. Wandel, G. Antesberger, S. Teuber, M. Vorwerk, A. Frangen, F. Katzwinkel, "193-nm immersion photomask image placement in exposure tools", Proc. SPIE 6154 (2006)
6. J. G. Doh, et al., "Feasibility study of mask fabrication in double exposure technology", Proc. SPIE 6349, (2006)
7. D-Y. Lee, et al., "Impact of the registration error of reticle on total overlay error budget", Journal of Vacuum Science and Technology B, Vol. 24, No. 6, pp. 3105-3109, 2006
8. H. J. Levinson, *Principles of Lithography*, 2005
9. M. Adel, M. Ghinovker, J. Paplowski, E. Kassel, P. Izikson, I. Pollentier, P. Leray, D. Laidler, "Characterization of overlay mark fidelity", Proc. SPIE 5038, 437 (2003)
10. B. Alles, B. Simeon, E. Cotte, T. Wandel, B. Schulz, R. Seltmann, "An empirical approach addressing the transfer of mask Placement errors during exposure", EMLC 2007 to be published
11. D. Choi, A. Jahnke, K. Schumacher, M. Hoepfl, "Overlay improvement by non-linear error correction and non-linear error control by APC", Proc. SPIE 6152, 61523W (2006)